J Mater Sci: Mater Electron
DOI 10.1007/s10854-016-4585-3

Control of crystal phase of $BiVO_4$ nanoparticles synthesized by microwave assisted method

Nguyen Dang Phu[1] · Luc Huy Hoang[1] · Phạm Khac Vu[1] · Meng-Hong Kong[2] · Xiang-Bai Chen[2] · Hua Chiang Wen[3] · Wu Ching Chou[3]

Received: 15 November 2015 / Accepted: 23 February 2016

Abstract Different crystalline phases $BiVO_4$ nanoparticles (tetragonal-zircon, monoclinic-scheelite, and tetragonal-zircon/monoclinic-scheelite heterophase) have been prepared by fast microwave assisted method and annealing treatment. For the heterophase, the ratio of tetragonal-zircon and monoclinic-scheelite phases can be well controlled by controlling the annealing temperature. Furthermore, a tight interface junction has been formed between tetragonal-zircon $BiVO_4$ and monoclinic-scheelite $BiVO_4$ in a nanosize level. This tight interface junction can modify the electronic structure of $BiVO_4$ nanoparticles, which would be very helpful for achieving high photocatalytic activity.

1 Introduction

Bismuth vanadate ($BiVO_4$) has attracted considerable attention due to its interesting ferroelastic, acoustooptical, and ion conductive properties [1–3]. In recent years, $BiVO_4$ is extensively studied for its promising photocatalytic applications such as pollutant decomposing and water splitting under visible light irradiation [4–9]. The properties of $BiVO_4$ strongly depend on its crystal phase. There are three main crystalline phases of $BiVO_4$ [7]: tetragonal zircon (z-t), tetragonal scheelite (s-t), and monoclinic scheelite (s-m). Generally, the z-t and s-m forms can exist at room temperature, while the s-t form exists at high temperatures. The room temperature z-t phase can irreversibly transform into s-m phase when heated up to 400–500 °C. The room temperature s-m phase can transform into s-t phase when heated up to 255 °C, and this transformation is reversible [1]. For photocatalytic applications, the reported studies have shown that s-m $BiVO_4$ has higher photocatalytic activity than z-t $BiVO_4$, and z-t/s-m heterophase would be more promising than single s-m phase [7–9]. Therefore, it is of great importance to achieve easy control of crystal phase of $BiVO_4$, for studying its interesting strong phase dependent properties and achieving high photocatalytic activity visible light driven catalyst.

Various methods have been applied to synthesize $BiVO_4$ crystallites, such as aqueous process, hydrothermal process, sonochemical method, and solid-state reaction method, etc. [10–14]. Generally, s-m $BiVO_4$ can be obtained by high-temperature processes, whereas z-t $BiVO_4$ can be prepared by low-temperature processes. In recent years, microwave assisted method has been widely used to synthesis nanomaterials due to the advantages of short reaction time, energy saving, high reaction rate, and easy forming of complex oxides at low temperatures [15]. In this paper, we show that good crystalline quality z-t $BiVO_4$ nanoparticles can be synthesized by fast microwave assisted method; and with further annealing treatment, good crystalline quality z-t/s-m heterophase and s-m phase can be obtained. For the heterophase, the ratio of z-t and s-m phases can be well controlled by annealing treatment,

✉ Luc Huy Hoang
hoanglhsp@hnue.edu.vn

✉ Xiang-Bai Chen
xchen@wit.edu.cn

[1] Faculty of Physics, Hanoi National University of Education, 136 Xuan Thuy, Cau Giay, Hanoi, Vietnam

[2] School of Science and Laboratory of Optical Information Technology, Wuhan Institute of Technology, Wuhan 430205, China

[3] Department of Electrophysics, National Chiao Tung University, Hsin-Chu 30010, Taiwan

Published online: 29 February 2016

and a tight interface junction has been formed between the two phases.

2 Experimental

The chemicals ammonium metavanadate (Merck) and bismuth nitrate (Merck) were of analytical grade and used as received. In a typical preparation, 5 mmol of ammonium metavanadate (NH_4VO_3) and 5 mmol of bismuth nitrate ($Bi(NO_3)_3{\cdot}5H_2O$) were dissolved in 100 ml of distilled water by stirring for 30 min at room temperature. The obtained solution was injected to a reaction vial with filling volume of 150 ml. The reaction vail was heated by a Sanyo microwave oven with power of 700 W to 110 °C for 20 min at atmosphere pressure. After microwave processing, the solution was cooled to room temperature. The resulted precipitates were separated by centrifugation, then washed with distilled water and ethanol for several times, and finally dried in an oven at 70 °C for 24 h. The as-prepared sample was then annealed in air at temperatures of 200, 300, 325, 350, 375, and 400 °C for 5 h.

The crystallography of the nanoparticles was analyzed using a Bruker D5005 X-ray diffractometer (XRD). The Raman scattering was performed using a Jobin–Yvon T64000 micro-Raman system in the back scattering geometry with a 671 nm laser excitation. The morphology of the nanoparticles was observed by scanning electron microscope (SEM, S4800-Hitachi). High resolution transmissions electron microscopy (HRTEM) images were conducted on a JEOL 2010 electron microscope operated at 200 kV. The UV–Vis diffuse reflectance (DRS) was performed using a Jasco V670 spectrophotometer.

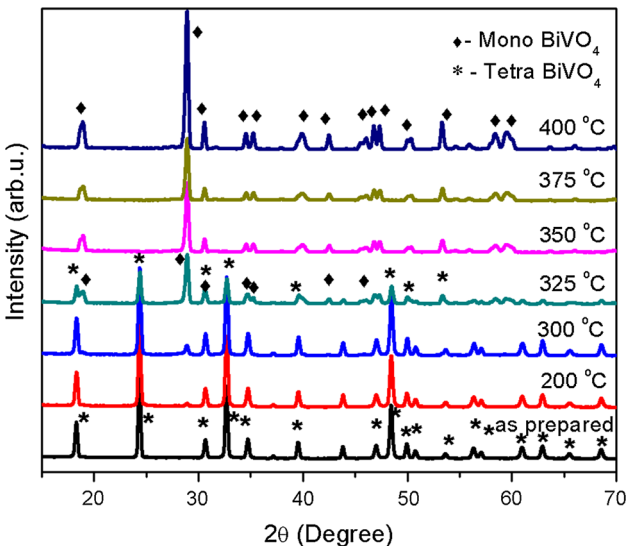

Fig. 1 XRD patterns of the as-prepared and thermally annealed samples

3 Results and discussion

Figure 1 shows the XRD patterns of the as-prepared and thermally annealed samples. The XRD results indicate that all the obtained $BiVO_4$ nanoparticles were well crystallized. The as-prepared sample can be well indexed to z-t $BiVO_4$ with the presence of characteristic diffraction peaks of (2 0 0), (112), (312), etc. (JCPDS 14-0133). The $BiVO_4$ samples annealed above 350 °C can be well indexed to s-m $BiVO_4$ with the presence of characteristic diffraction peaks of (121), (004), etc. (JCPDS 75-1867). When annealed above 400 °C, the intensity of all the diffraction peaks of s-m $BiVO_4$ shows a clear increase, indicating better crystalline quality nanoparticles can be obtained with annealing above 400 °C.

The $BiVO_4$ samples annealed from 200 to 325 °C are of heterophase including both z-t and s-m phases. The percentage of s-m phase can be roughly estimated from the normalized ration of relative intensities for the (1 2 1) peak of s-m phase against that for the (2 0 0) peak of z-t phase [16]:

$$V_{s-m} = \frac{I_{s-m(121)}}{I_{s-m(121)} + I_{z-t(200)}}$$

where $V_{\text{s-m}}$, $I_{\text{s-m(121)}}$, and $I_{\text{z-t(200)}}$ denote the percentage of s-m phase, the relative intensity of (1 2 1) peak for s-m

Table 1 Effects of annealing temperature on crystalline phases and optical bangap of $BiVO_4$ nanoparticles

Sample	Annealing temperature (°C)	Percentage of s-m phase (%)	E_g, z-t phase (eV)	E_g, s-m phase (eV)
1	As-prepared	0	2.85	–
2	200	3	2.83	2.51
3	300	8	2.75	2.45
4	325	60	2.74	2.42
5	350	100	–	2.40
6	375	100	–	2.40
7	400	100	–	2.40

phase and that of (2 0 0) peak for z-t phase, respectively. We estimated that the percentage of the s-m phase is about 3, 8, and 60 % for the $BiVO_4$ samples annealed at 200, 300, and 325 °C, respectively (Table 1).

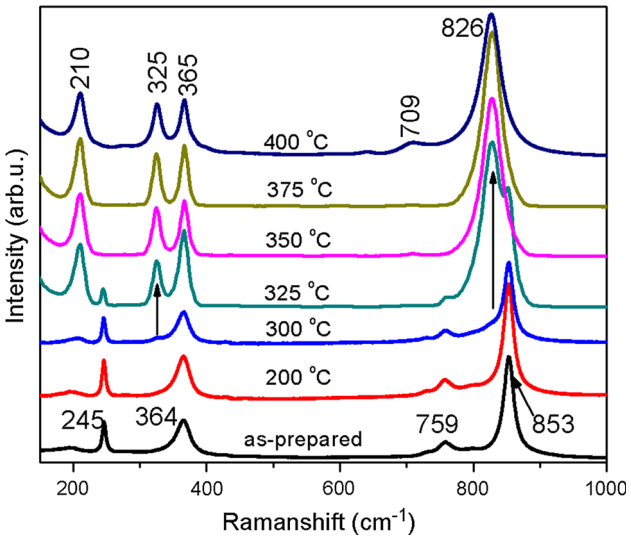

Fig. 2 Raman scattering spectra of the as-prepared and thermally annealed samples

The identity of crystal phases of the $BiVO_4$ samples was further confirmed by Raman study. Figure 2 shows the Raman spectra of the as-prepared and thermally annealed samples. For the as-prepared sample, four Raman peaks at 850, 759, 364, and 245 cm^{-1} can be clearly observed. These four peaks agree well with the symmetric V–O stretching mode (A_g symmetry), antisymmetric V–O stretching mode (B_g symmetry), O–V–O bending mode (A_g symmetry), and Bi–O stretching mode (E_g symmetry) of z-t $BiVO_4$. For the $BiVO_4$ nanoparticles obtained with annealing temperature above 350 °C, the Raman modes observed in the z-t phase disappeared, and four new intense Raman peaks at 826, 365, 325, and 210 cm^{-1} are clearly observed, which are characteristic vibrational modes of s-m $BiVO_4$ [17]. The peak at 826 cm^{-1} can be assigned to symmetric V–O stretching mode (A_g). The peaks at 365 and 325 cm^{-1} can be assigned to symmetric V–O bending mode (A_g) and antisymmetric V–O bending mode (B_g) of VO_4 units, respectively. The peak at 210 cm^{-1} can be assigned to external mode (rotation/translation). For the $BiVO_4$ nanoparticles obtained with annealing of 400 °C, in addition the above four intense peaks, a weak Raman peak at 709 cm^{-1} is observed, which can be assigned to antisymmetric V–O stretching mode (B_g) of s-m phase. The Raman results further confirms that the as-prepared sample is of z-t phase; with annealing above 350 °C, single

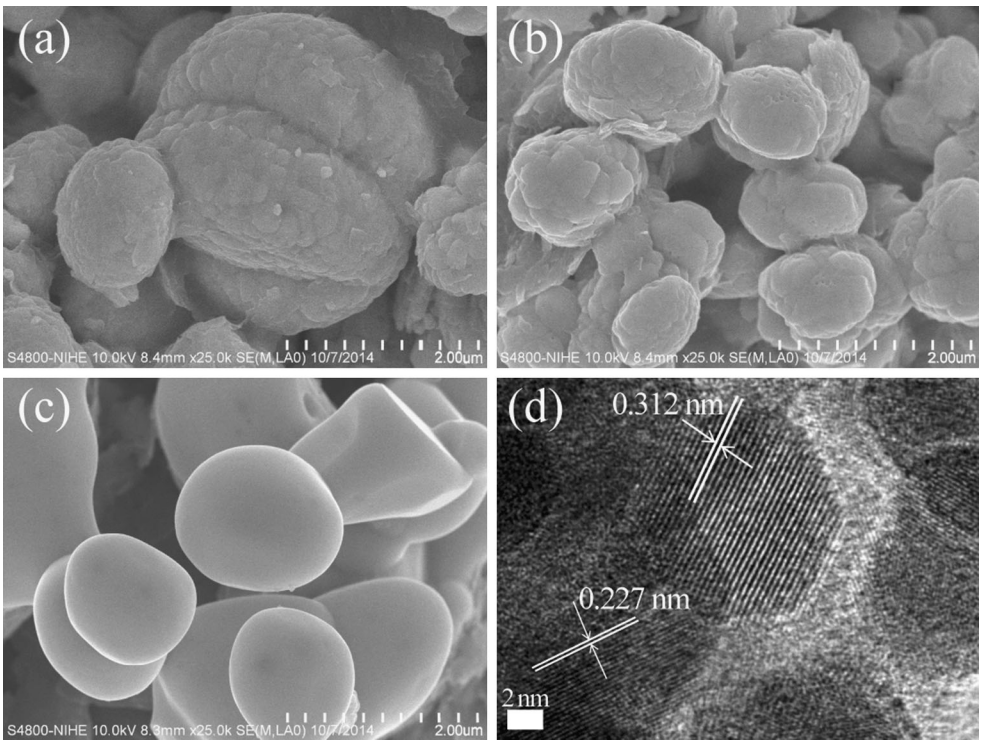

Fig. 3 FESEM images of the samples as-prepared (**a**), annealed at 325 °C (**b**), and 400 °C (**c**), **d** is the HRTEM image of the sample annealed at 325 °C

s-m phase can be obtained, and with annealing above 400 °C, the crystalline quality of s-m $BiVO_4$ can be improved. These are in good agreement with XRD results in Fig. 1.

For the as-prepared sample, a very weak Raman peak at 200 cm^{-1} is also observed. With annealing of 200 and 300 °C, the peak intensity slowly increases and peak position shows blueshift. With further increasing annealing temperature to 325 °C, the peak intensity shows a quick increase and peak position further blueshifts to 210 cm^{-1}. The Raman results indicate that in the as-prepared sample, the content of s-m phase would be significantly below 3 % therefore not detectable by XRD measurement. Consistent with the XRD results, the Raman results also suggested that with annealing below 300 °C, only a few percent z-t $BiVO_4$ is transformed into s-m $BiVO_4$; the significant phase transition occurs 325 °C, at this temperature 60 % percent z-t $BiVO_4$ can be transformed into s-m $BiVO_4$.

The morphology of the samples was revealed by field emission scanning electron microscopy (FESEM). Figure 3a–c present the FESEM images of the samples as-prepared, annealed at 325 and 400 °C, respectively. The FESEM images indicate that the $BiVO_4$ nanoparticles are mainly sphere like particles with crystalline size of about several hundred nanometers. The FESEM image showed that with 400 °C annealing, the surface morphology of nanoparticles is clearly improved, indicating better crystalline quality. This is consistent with XRD and Raman results. Importantly, the FESEM showed that in the heterophase $BiVO_4$, the nanoparticles are closed packed, which may indicates that a tight interface junction could be formed between z-t $BiVO_4$ and s-m $BiVO_4$ in a nanosize level. The tight interface junction is also indicated by the high-resolution transmission electron microscopy (HRTEM) image of heterophase $BiVO_4$ nanoparticles, as presented in Fig. 3d. The lattice spacing of 0.312 nm corresponds to the (103) crystalline plane of s-m $BiVO_4$, whereas the fringe of 0.227 nm matches the (301) crystallographic plane of z-t $BiVO_4$. Furthermore, to be discussed below, the absorption spectra also suggest that a tight interface junction would be formed between z-t $BiVO_4$ and s-m $BiVO_4$ in a nanosize level. The formation of tight interface junction between two phases may helpful for separation of photogenerated charge carriers, thus achieving high photocatalytic activity.

Figure 4 presents the UV–Vis diffuse reflectance (DRS) spectra of the as-prepared and thermally annealed samples. As can be seen from Fig. 4, with the phase transition from z-t $BiVO_4$ to s-m $BiVO_4$, the absorption spectra varied in an ordered fashion. The as-prepared sample showed a steep absorption 450 nm and a tail absorption 500 nm. Similar tail absorption was also observed by Zhang et al. [18], which suggested that the tail absorption may result from the crystal defects formed during the growth of $BiVO_4$

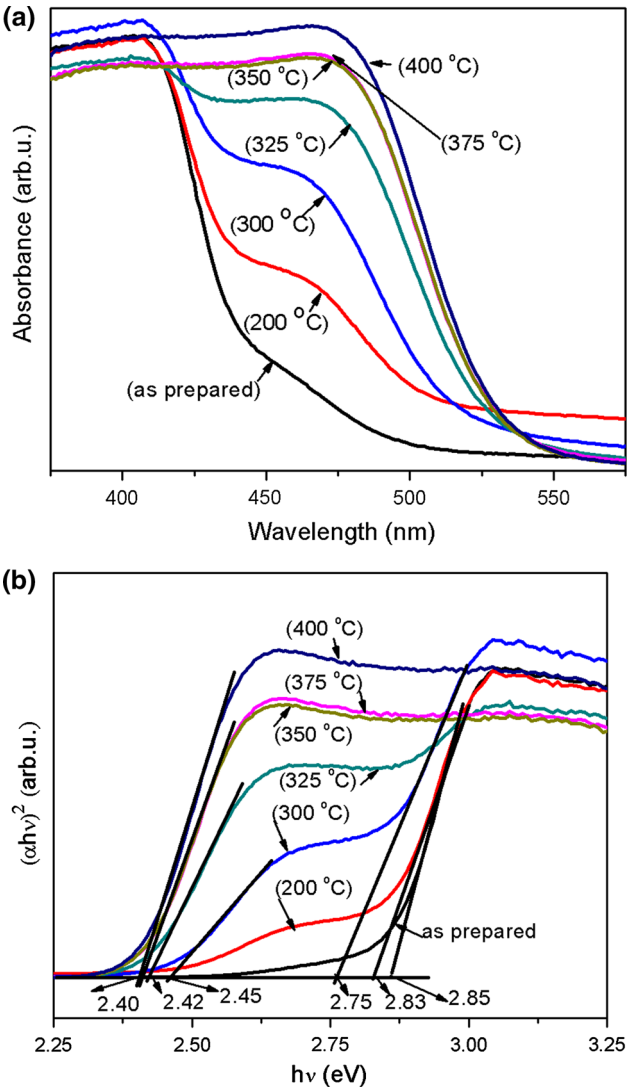

Fig. 4 **a** Reflectance diffusion spectra, and **b** plots of $(\alpha h\nu)^2$ vs photon energy (hν), of the as-prepared and thermally annealed samples

nanoparticles. Our results indicate that the weak tail absorption would be correlated with very small amount of s-m phase in the as-prepared sample.

A steep absorption would indicate bandgap transition. For a crystalline semiconductor, the band edge absorption follows the formula $\alpha h\upsilon = A(h\upsilon - Eg)^{n/2}$, where α, h, υ, Eg, and A are absorption coefficient, Planck constant, light frequency, bandgap, and a constant, respectively [19, 20]. For direct band gap semiconductor $BiVO_4$, n equals 1 [12]. The bandgap Eg can be estimated from a plot $(\alpha h\nu)^2$ versus photon energy (hν): the intercept of the tangent to the x-axis gives a good approximation of Eg [21]. Plots of $(\alpha h\nu)^2$ versus photon energy (hν) of the samples are shown in Fig. 4b. The estimated bandgap of as-prepared z-t $BiVO_4$ is 2.85 eV. With annealing of 200 and 300 °C, the

bandgap of z-t $BiVO_4$ redshifts to 2.83 and 2.75 eV, respectively. With annealing above 350 °C, the z-t $BiVO_4$ disappears, and s-m $BiVO_4$ with bandgap of 2.40 eV is obtained (Table 1). Also, the bandgap of s-m $BiVO_4$ has a redshift with increasing annealing temperature.

It is well known that the electronic structure of the semiconductor usually plays a crucial role in its photocatalytic activity. The absorption spectra clearly demonstrate that the electronic structures of $BiVO_4$ nanoparticles are gradually modified by the annealing treatment. In addition, the absorption spectra show that with increasing annealing temperature, the absorption contribution from s-m phase has a quick increase, even at annealing temperature of 200 and 300 °C, very different with XRD and Raman results. This indicates that for heterophase $BiVO_4$, its electronic structure is also modified by the interaction between z-t $BiVO_4$ and s-m $BiVO_4$. This is consistent with the FESEM and HRTEM images, which indicated that a tight interface junction would be formed between z-t $BiVO_4$ and s-m $BiVO_4$ in a nanosize level. The modification of electronic structure of $BiVO_4$ nanoparticles would be of great importance for achieving high photocatalytic activity. A study of the photocatalytic activity of the $BiVO_4$ nanoparticles is currently underway and will be reported in a later paper.

4 Conclusion

A series of different crystalline phases $BiVO_4$ nanoparticles (z-t, s-m, and z-t/s-m heterophase) have been prepared by fast microwave assisted method and annealing treatment. The XRD and Raman results showed that for the heterophase, the ratio of z-t $BiVO_4$ and s-m $BiVO_4$ can be well controlled. The electron microscopy and absorption results indicated that a tight interface junction has been formed in the heterophase $BiVO_4$ nanoparticles. The formation of tight interface junction in nanoscale can modify the electronic structure of $BiVO_4$ nanoparticles, which would be crucial for achieving high photocatalytic activity.

Acknowledgments The authors would like to thank the Vietnam's National Foundation for Science and Technology Development (NAFOSTED), Grant 103.02-2013.51 for financial support. X. B. Chen acknowledges the support by Wuhan Institute of Technology.

References

1. A.R. Lim, K.H. Lee, S.H. Choh, Solid State Commun. **83**, 185–186 (1992)
2. S.V. Akimov, I.E. Mnushkina, E.F. Dudnik, Sov. Phys. Technol. Phys. **27**, 500–503 (1982)
3. K. Hirota, G. Komatsu, M. Yamashita, H. Takemura, O. Yamaguchi, Mater. Res. Bull. **27**, 823–830 (1992)
4. X. Zhang, Z.H. Ai, F.L. Jia, L.Z. Zhang, X.X. Fan, Z.G. Zou, Mater. Chem. Phys. **103**, 162–167 (2007)
5. K. Sayama, A. Nomura, T. Arai, T. Sugita, J. Phys. Chem. B **110**, 11352–11360 (2006)
6. B.P. Xie, H.X. Zhang, P.X. Cai, R.L. Qiu, Y. Xiong, Chemosphere **63**, 956–963 (2006)
7. H.M. Fan, T.F. Jiang, H.Y. Li, D.J. Wang, L.L. Wang, J.L. Zhai, D.Q. He, P. Wang, T.F. Xie, J. Phys. Chem. C **116**, 2425–2430 (2012)
8. G.C. Xi, J.H. Ye, Chem. Commun. **46**, 1893–1895 (2010)
9. Y. Wang, J. Huang, G. Tan, J. Huang, L. Zhang, NANO **10**, 1550008 (2015)
10. A. Kudo, K. Omori, H. Kato, J. Am. Chem. Soc. **121**, 11459–11467 (1999)
11. S. Obregón, A. Caballero, G. Colón, Appl. Catal. B **117**–**118**, 59–66 (2012)
12. L. Zhou, W. Wang, S. Liu, L. Zhang, H. Xu, W. Zhu, J. Mol. Catal. A Chem. **252**, 120–124 (2006)
13. A.W. Sleight, H.Y. Chen, A. Ferretti, D.E. Cox, Mater. Res. Bull. **14**, 1571–1581 (1979)
14. K. Soma, A. Iwase, A. Kudo, Catal. Lett. **144**, 1962–1967 (2014)
15. S.E. Ela, S. Cogal, S. Icli, Inorg. Chim. Acta **362**, 1855–1858 (2009)
16. A.K. Bhattacharya, K.K. Mallick, A. Hartridge, Mater. Lett. **30**, 7–13 (1997)
17. R.L. Frost, D.A. Henry, M.L. Weier, W.J. Martens, Raman Spectrosc. **37**, 722–732 (2006)
18. A. Zhang, J. Zhang, N. Cui, X. Tie, Y. An, L. Li, J. Mol. Catal. A Chem. **304**, 28–32 (2009)
19. M.A. Butler, J. Appl. Phys. **48**, 1915–1920 (1997)
20. Z.F. Zhu, J. Du, J.Q. Li, Y.L. Zhang, D.G. Liu, Ceram. Int. **38**, 4827–4834 (2012)
21. J.G. Yu, J.C. Yu, W.K. Ho, Z.T. Jiang, New J. Chem. **26**, 607–613 (2002)